Article

Dynamic optimization of a subcritical steam power plant under time-varying power load

Chen Chen [1] and George M. Bollas [2]*

[1] Department of Chemical & Biomolecular Engineering, University of Connecticut, 191 Auditorium Road, Unit 3222, Storrs, CT 06269, USA; chen.chen@uconn.edu
[2] Department of Chemical & Biomolecular Engineering, University of Connecticut, 191 Auditorium Road, Unit 3222, Storrs, CT 06269, USA; george.bollas@uconn.edu
* Correspondence: george.bollas@uconn.edu; Tel.: +1-860-486-6037

Abstract: The increasing variability in power plant load, in response to a wildly uncertain electricity market and the need to to mitigate CO_2 emissions, lead power plant operators to explore advanced options for efficiency optimization. Model-based, system-scale dynamic simulation and optimization are useful tools in this effort, and the subject of the work presented here. In prior work, a dynamic model validated against steady-state data from a 605 MW subcritical power plant was presented. This power plant model is used as a test-bed for dynamic simulations, in which the coal load is regulated to satisfy a varying power demand. Plant-level control regulates plant load to match an anticipated trajectory of the power demand. The efficiency of the power plant operating at varying load is optimized through a supervisory control architecture that performs set point optimization on the regulatory controllers. Dynamic optimization problems are formulated to search for optimal time-varying input trajectories that satisfy operability and safety constraints during the transition between plant states. An improvement in time-averaged efficiency of up to 1.8% points is shown feasible with corresponding savings in coal consumption of 184.8 tons/day and carbon footprint decrease of 0.035 kg/kWh.

Keywords: Power plants, supervisory control, dynamic simulation, dynamic optimization

1. Introduction

The excessive emissions of CO_2 from fossil-fueled power plants contribute to the greenhouse effect and global warming. Increasing the efficiency of power generation cycles and integration with CO_2 capture units, are nowadays accepted as the most promising short-term approaches to reducing CO_2 emissions while we transition to renewable and carbon free energy sources [1,2]. Efficiency improvements can be achieved through the optimization of power plant operating strategies or modification of the plant design. For instance, new fossil-fueled power plants use a combination of steam and gas turbines to generate electricity, resulting in thermal efficiencies as high as 61% [3]. Moreover, modern coal-fired Rankine cycle systems can achieve efficiencies as high as ~47%, using ultra-supercritical boilers [4]. For instance, the commercial power plant of Lünen (Germany) burns low-sulfur hard coal [5], at an efficiency up to 46%, in a 750 MW ultra-supercritical once-through boiler, operating at steam conditions of 600°C and 280 bar [6]. Nonetheless, subcritical coal-fired steam power plants that operate on the principle of the Rankine Cycle still serve more than 1/3 of the electricity demand in the U.S. [7]. Subcritical power plants, operating at pressure lower than 220 bar, have a nominal efficiency of 37% [8]. Compared to supercritical and ultra-supercritical plants, the more common subcritical plants are advantageous in terms of lower installation costs, operating and maintenance experience [5,7]. Therefore, optimization of the efficiency of subcritical power plants is the first realistic step in our efforts to reduce CO_2 emissions from the power sector.

Due to seasonal and daily fluctuations in power demand, and new deployment programs focused on renewable energy, dynamic simulation and optimization are required for power plants in order to

respond to the resulting time-varying power demand. The contribution of electricity generation from renewable energy sources in the world will expand from the current 21% to 29.8% in 2040 [7]. The impact of this increase in penetration of renewable sources has been explored by many researchers. For example, Shah et al. [9] showed that the higher penetration of large-scale photovoltaic plants in the power grid will lead to significant variations in the power flow across the grid and unstable power generation profiles for the balancing conventional plants. The work by Edmunds et al. [10] showed that today's power plants are subject to more intense ramping operations, due to the increasing variable renewable penetration. Critz et al. [11] focused on the challenges arising from the inability to accurately forecast renewable power generation. Correspondingly, Eser et al. [12] showed that the high penetration of renewable energy sources will result in an increase of periodic start-ups of thermal power plants. Thus, the simulation of the dynamic behavior of the integrated electricity sector and in particular the dynamicity of the fossil-fueled power plants, which will provide the balance power (between renewables input and market demand) is increasingly of interest to improve productivity and stability, and reduce cost and emissions.

The efficiency of conventional fossil–fueled power plants that are based on the Rankine Cycle mostly depends on the steam temperature and pressure [4], with the majority of previous work on efficiency optimization of these plants focusing on steady-state analyses. The work by Fu et al. [13] showed an average efficiency increase of 0.1% points for every increment of 8°C in boiler feedwater temperature, every decrement of 4.5°C in flue gas temperature, and every increment of 10 bar in main steam pressure, compared to a reference case with an efficiency of 45.5%. Sanpasertparnich and Aroonwilas [14] presented potential efficiency improvements of up to 8.88% points for subcritical coal-fired power plants. They identified the preheated air temperature, main steam temperature and the pressure of streams extracted from the high-, intermediate-, and low-pressure turbines (HP, IP and LP, respectively), as the most critical variables in the optimization of power plant performance. In the work by Tzolakis et al.[15], an absolute net efficiency gain of 0.55% was shown to be feasible, by reducing the mass flow rate of the steam exiting the HP turbines and increasing the mass flow rate of the steam exiting the IP and LP turbines. These significant efforts in the area of steady-state optimization of power plants paved future work on dynamic optimization. Moreover, advancements in process modeling tools, such as Dymola [16] and gPROMS [17], have made it easier to simulate these processes dynamically. For instance, Chen et al.[18] developed a Dymola [16] dynamic model of a combined cycle power plant integrated with chemical-looping combustion, with the combustion process optimized in gPROMS [17] to maximize the power plant efficiency. Franke et al. [19] presented a model-based, dynamic optimization framework exploiting the Modelica language [20] for improving power plant performance. Their work illustrated efficiency benefits from applying offline optimization results to online power plant operations. Lind and Sallberg [21] used modern acausal simulation and optimization tools to optimize the start-up procedure of a combined cycle power plant. Their analysis showed that the thermal stress in the heat recovery steam generator is the major constraint limiting the rapid start-up of the gas turbines to full load.

One practical approach to improve the efficiency of existing fossil-fueled power plants is to deploy supervisory control schemes targeted to efficiency optimization. Supervisory control architectures are often used to perform tasks of process optimization without changing the plant infrastructure and design. Skogestad [22] presented a systematic procedure for designing advanced control structures at the supervision level for complex chemical plants. The critical first steps in designing a supervisor logic are to define the operational and economic objectives and the available degrees of freedom. Common degrees of freedom include the set points of the regulatory controllers, system boundaries not controlled and system parameters tunned to a particular operating scheme. For instance, Lestage et al. [23] presented linear supervisory control designs for constrained real-time optimization of an ore grinding plant, in which they optimized the set points of the local controllers, to maximize throughput. Baillie and Bollas [24] presented the key steps in the development of a high-fidelity model for a chiller plant which was used in supervisory resilient control architectures for plant optimization under fault

scenarios by Mittal et al. [25]. Obviously, supervisory control is a promising approach for efficiency optimization of power plants, wherein there exists a large number of regulatory controllers, which must be maintained for safety and performance reasons. In one such effort, Sáez et al. [26] developed a supervisory algorithm based on adaptive predictive control to optimize the operation of the gas turbine of a combined cycle power plant in Chile. They showed the potential of 3% fuel consumption savings, by manipulating variables such as the fuel flow, air flow and steam flow. Ponce et al. [27] presented a dynamic simulator of an integrated solar combined cycle power plant, incorporating a supervisory control strategy. Fuel savings of 1.7%∼3.7% were shown feasible, by manipulating the set points of the regulatory controllers of the steam pressure, gas turbine power and steam turbine power. These efforts focused mostly on the optimization of a few power plant components instead of solving a problem that maximizes the power plant efficiency using all or most of the degrees of freedom. In this work, the optimization problem serving the supervisory controller deals with the integrated coal-fired steam power plant.

In prior work [28], a power plant model was developed and validated against steady-state data from a fossil-fueled subcritical power plant with a reheat, regenerative cycle [29]. The power plant modeled exhibits full-load power generation of 605 MW at efficiency of 38.7%. Conventional proportional-integral-derivative (PID) controllers were incorporated into the system model. Dynamic simulation of the power plant operating with step changes in fuel load, showed that the controllers are robust in maintaining the controlled variables at set point. In this work, open-source data of time-varying power demand along with its forecast from the New England area are used to study this plant at realistic operating conditions [30]. A fuel load controller is implemented to meet the time-varying power demand, and controllers are added to adjust the air flow and water flow for time-varying load. Supervisor control strategies are applied for static and dynamic optimization of the power plant efficiency. This optimization is accomplished by manipulating the set points of the regulatory controllers of the temperature of the superheated steam and preheated air, and the mass flow rates of steam extracted from the steam turbines. Steady state and dynamic optimization results are compared and discussed in an effort to explore the value proposition of each.

2. Power plant studied and plant model

The power plant studied and simulated in prior work [28] was the fossil fuel-fired subcritical power plant shown in Figure 1, with operating conditions at full load as reported by Singer [29]. The plant employs a reheat, regenerative cycle to produce 605 MW electricity by burning fossil-fuel, with nominal turbine conditions of 174 bar and 538°C steam. Combustion of bituminous B coal [5] with preheated air produces hot flue gas that evaporates and superheats water. The feedwater is converted to high temperature superheated steam, through a series of heat exchange steps in the boiler, including the Economizer, Evaporator, Reheater, and Superheater. The superheated steam produced in the boiler is expanded in a series of high-pressure (HP), intermediate-pressure (IP) and low-pressure (LP) turbines connected to a generator to convert the heat to mechanical torque and produce electricity. The steam exiting the last LP turbine is condensed in the Condenser. The condensate is preheated in four heat exchange steps, including a deaerator and three water preheaters, which are supplied with steam streams extracted from the HP, IP, and LP turbines. Three pumps, namely the condensate booster pump, condensate pump and boiler feed pump, are used for re-circulating the water after being condensed in the condenser. The preheated condensate re-enters the boiler at high pressure and closes the loop.

Preprints (www.preprints.org) | NOT PEER-REVIEWED | Posted: 5 June 2018 doi:10.20944/preprints201806.0052.v1

Peer-reviewed version available at Processes 2018, 6, 114; doi:10.3390/pr6080114

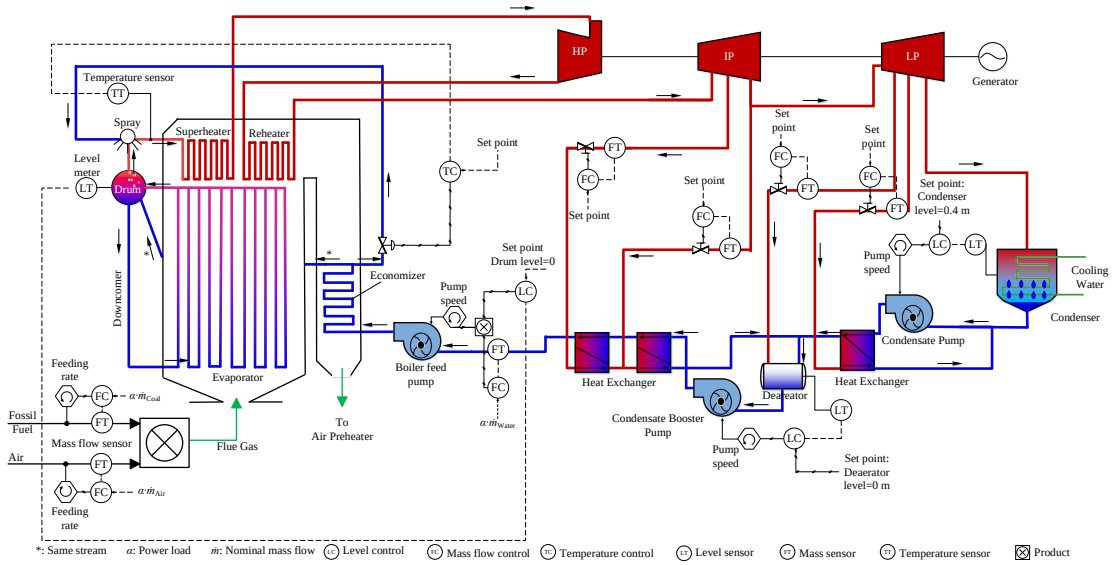

Figure 1. Reheat regenerative cycle, 605 MW subcritical-pressure fossil power plant with control system design [29].

The plant of Figure 1 was simulated with a dynamic power plant model developed in Dymola [16] using the Modelon ThermalPower library [31]. The Modelica language used in Dymola is a non-proprietary, object-oriented, equation-based language for the modeling of complex physical systems [20], well-suited for the objective of large-scale dynamic simulation of power plants. A comprehensive list of the operating data of the power plant was provided in prior work, and the plant model was provided as Supporting Information to that work [28]. The model of the plant operating at full load was shown to be in excellent agreement with steady state data from the reference power plant. Figure 1 also shows the design of the control system of that plant, including controllers for safety regulation (marked with black solid lines), plant-level controllers (marked with blue dashed lines), and controllers for plant optimization (marked with red dotted lines). The regulatory control system, including the controllers of superheated steam temperature, and of the water level in the Drum, Condenser and Deaerator, was discussed in detail in prior work [28]. This regulatory control system was tunned using bump tests and the dynamic responses of the model were assessed qualitatively in terms of robustness and plant stability. The multilayer control scheme designed in this work and the controllers required to meet the time-varying power load are discussed in the following.

3. Power plant under time-varying power demand

Extensive studies of the power demand and its forecasting have resulted in excellent models of the power demand per market sector, such as gray-box prediction models, to forecast real-time electricity demand with an error less than 8% [32,33]. The forecasted power demand is typically used by utility companies to predict the grid load and maintain service reliability. In this work, the data of power demand (along with its forecast) in the New England area were used. In particular, the data of the day of April 17, 2016 was used as a realistic sample of power demand fluctuations [30]. The duration for the temporal forecasted power demand studied was 24 hours. To meet the full power load of the reference power plant (605MW), the ISO New England data (maximum value is 18000 MW) was uniformly scaled–down, as shown in Figure 2 (a). The underlying assumption in this normalization was that the power demand from one power plant is proportional to the total power consumed. Therefore, it was considered that a fraction of the total power demand (scaled by a constant factor) and its daily fluctuation need to be met by one power plant. The reality with renewable inputs in the grid is, as mentioned, a more abruptly fluctuating load for the power plant. It is thus anticipated

Preprints (www.preprints.org) | NOT PEER-REVIEWED | Posted: 5 June 2018 doi:10.20944/preprints201806.0052.v1

Peer-reviewed version available at Processes 2018, 6, 114; doi:10.3390/pr6080114

that the efficiency gains from the analysis presented herein are a lower bound to the potential efficiency gains when renewable energy becomes a more dominant contribution to the electric grid.

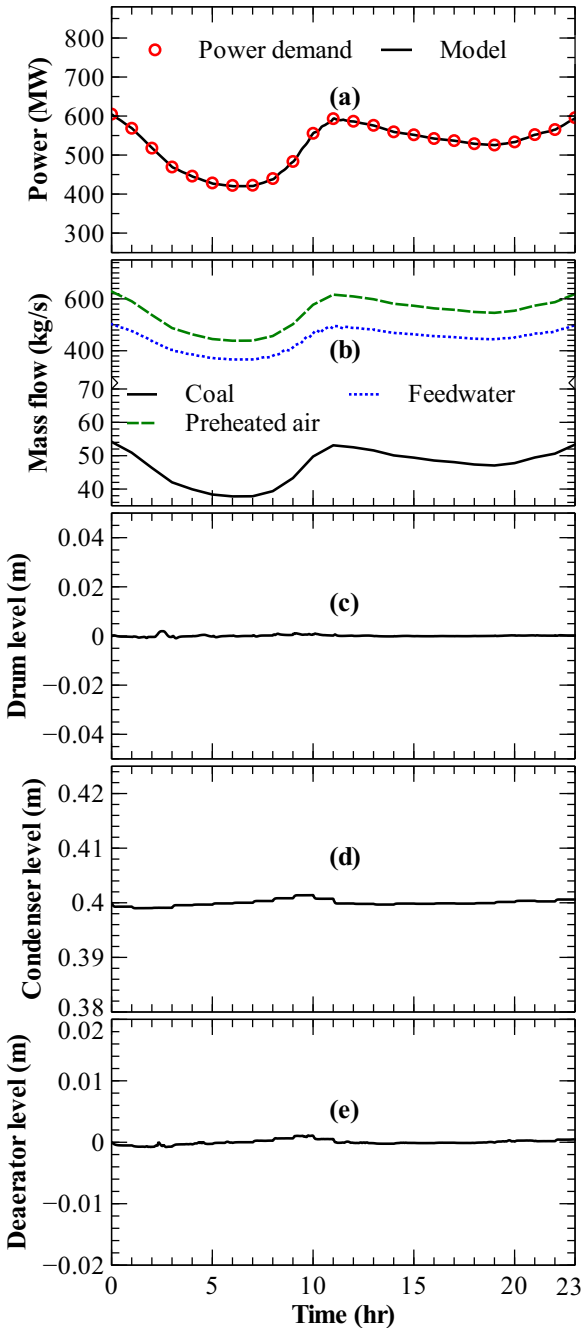

Figure 2. Dynamic performance of the power plant model: (a) power demand and power generated by the plant model; (b) mass flow rates of coal, preheated air and feedwater; (c) water level in the Drum; (d) water level in the Condenser; (e) water level in the deaerator.

In prior work [28], the power plant model was validated dynamically, showing fast responses to sudden changes in coal load. The regulatory control system incorporated in the power plant model was shown to be robust in maintaining controlled variables at set points. Here, plant-level controllers were added to the plant model, as shown in Figure 1, to adjust the coal load, preheated air flow and feedwater flow so that the plant meets the time-varying power load of Figure 2(a). The mass flow rate of feedwater ($\dot{m}_{FW}$) circulating in the plant and the mass flow rate of prehreated air ($\dot{m}_{Air}$) mixed with

Preprints (www.preprints.org) | NOT PEER-REVIEWED | Posted: 5 June 2018 doi:10.20944/preprints201806.0052.v1

Peer-reviewed version available at Processes 2018, 6, 114; doi:10.3390/pr6080114

the fuel were assumed to be proportional to the power load [34]. The mass flow rates of feedwater and preheated air were set to adjust with plant load, by multiplying the nominal $\dot{m}_{Air}$ and $\dot{m}_{FW}$ by the temporal power load change ratio. The mass flow rate of coal was adjusted by a PID fuel load controller to match the temporal power demand. Table 1 presents the tunning parameters of the feedforward control of water and air feed rates and the PID controller of fuel load. The measurement for the fuel load controller is the power generation (P), the manipulated variable is the coal mass flow ($\dot{m}_{Coal}$), and the set point is the temporal profile of the normalized power demand of the New England area [30]. These new controllers were tuned following standard methodologies discussed elsewhere [28]. Figure 2(a) shows that the power generated by the plant model matches the power demand of the normalized New England area data [30]. Figure 2(b) shows the transient responses of $\dot{m}_{Coal}$, $\dot{m}_{Air}$ and $\dot{m}_{FW}$ to the dynamically varying power demand of Figure 2(a). Figures 2(c–e) show that the safety–critical regulated variables (water levels in the drum, condenser and deaerator) are robustly controlled, and exhibit negligible oscillations. The dynamic performance of the plant model over the entire 24-hour period suggests that the model provides a robust test-bed of the plant physics and its controls, and is used in the following for steady state and dynamic optimization.

Table 1. Controllers for the power plant in response to a time-varying power load.*

Feedforward control: Air and feedwater controllers				
Controlled variables	$\dot{m}_{Air}$	$\dot{m}_{FW}$		
PID control: Fuel load controller				
Controlled variables	Manipulated variables	K_p	K_i	K_d
P	$\dot{m}_{Coal}$	1e-8	1e-10	1e-6

* P: Power generation; $\dot{m}_{Air}$: Mass flow rate of air; $\dot{m}_{FW}$: Mass flow rate of feedwater; $\dot{m}_{Coal}$: Mass flow rate of coal; K_p: Coefficient of the proportional term; K_i: Coefficient of the integral term; K_d: Coefficient of the derivative term.

4. Optimization for an integrated power plant

4.1. Objective and Optimization Variables

The objective of plant-level optimization is to maximize the efficiency of the power plant while operating at steady state, or the integral of the efficiency over time if the power plant is operating in a transient fashion. This was accomplished by calculating optimal set points for the regulatory controllers, without violating operability and safety constraints. The plant efficiency was calculated as [29]:

$$\eta = \frac{P_{ST} - P_{Pumps}}{\dot{m}_{Coal} LHV_{Coal}} \tag{1}$$

where η is the efficiency of the plant, $\dot{m}_{Coal}$ is the mass flow rate of coal, LHV_{Coal} is the lower heating value of coal, P_{ST} is the power generated by steam turbines, and P_{Pumps} is the power consumed by pumps. Here, high-volatile bituminous B coal with an average LHV of 28 MJ/kg was used [5]. Other auxiliary energy losses were not not considered in Eq.(1), as previous work has shown that auxiliary efficiency losses are small, often of the order of ∼2 MW for coal-fired steam cycles for a plant size similar the one studied here [29,35]. As discussed in the introduction, the power plant efficiency of Eq.(1) can be improved by manipulating several plant variables. Table 2 summarizes the optimization variables, ranges of variability and the efficiency improvements achieved in relevant previous work. In the majority of previous analyses [13–15,36–44], plant efficiency optimization was performed by manipulating the temperature of superheated steam (T_{SH}). For example, Xiong et al. [41] showed that the higher superheated steam temperature increases the power generated by the HP turbine, improving cycle efficiency. Several other variables have been explored in the literature for their capability to improve plant efficiency. Sanpasertparnich et al. [14,36] presented the impact of preheated air temperature (T_{Air}) on power plant efficiency. Tzolakis et al. [15,42] optimized the

plant efficiency at full load, by manipulating the mass flow extracted from steam turbines ($\dot{\mathbf{m}}_{ST}$, which includes $\dot{m}_{HP}$, $\dot{m}_{IP}$ and $\dot{m}_{LP}$). Other optimization variables, such as the moisture content of coal [45], mass flow rate of feedwater [42], isentropic efficiency of turbines [41], temperature of flue gas exiting the boiler [43], and the pressure of steam extracted from turbines [14,36], require changes in the existing infrastructure, and were not considered here. In summary, the common plant efficiency optimization variables T_{SH}, T_{Air}, and $\dot{\mathbf{m}}_{ST}$ were chosen in this work. For the purpose of illustration, two optimization cases were considered. Case study I presents plant optimization by manipulating T_{SH} and T_{Air} within an operation horizon of 24 hours. Case study II presents plant optimization by manipulating $\dot{\mathbf{m}}_{ST}$ with an operation horizon of 4 hours. The inputs of each optimization problem are discussed in detail in the following.

Table 2. Review of power plant optimization efforts and respective variables.*

Ref.	$\Delta\eta$ (%)	Optimization variables						
		T_{SH} (°C)	$\dot{m}_{IP1}/\dot{m}_{IP2}$ $/\dot{m}_{LP1}/\dot{m}_{LP2}$ (kg/s)	T_{Air} (°C)	$\dot{m}_{FW}$ (kg/s)	p_{SH} (bar)	β (%)	Others
[14,36]	7.8	[530,600]	[3.9,19.6]/ [6.2,43.3]/ [15.1,28.7]/ [11.1,42.1]	[166,190]	[250,350]	[166,190]	[11.1,17.6]	
[15]	0.55		[0,30.8]/ [0,51.2]/ [0, 21.1]/ [0,0.94]					
[37]	0.41	[600,625]	[16,26]/ [14,24]/ [12.6,24]/ [34,57]		[400,475]	[20,30]		
[38,39]	2.8	[550,700]		[35,275]		[230,350]		Excess air$\in$[0,25%], T_{RH} $\in$[580,620]
[40]	2	[550,700]				[230,350]		η_{ST} $\in$[0.75,0.87], $p_{HP/IP/LP}$(bar) $\in$[60/9/0.0356, 80/25.5/2.68]
[13]	5.9	[487,1076]				[150,450]		
[41]	2.5	[535,545]						η_{ST} $\in$[0.8,0.95]
[42]	1.3	[485,537]			[45,57]			
[43]	0.79	[115,278]			[21,38.4]			T_{FG}(°C)$\in$[85,125]
[44]	3.5	[460,530]				[64,110]		p_{CON}(bar) $\in$[0.01,0.05]

* T_{SH}: Temperature of superheated steam; $\dot{m}_{HP}$: Mass flow rates of steam extracted from high-pressure turbine; $\dot{m}_{IP}$: Mass flow rates of steam extracted from intermediate-pressure turbine; $\dot{m}_{LP}$: Mass flow rates of steam extracted from low-pressure turbine; ; p_{SH}: Pressure of the superheated steam; T_{Air}: Temperature of the preheated air; $\dot{m}_{FW}$: Mass flow rate of feedwater; β: Coal moisture content; η_{ST}: Isentropic efficiency of steam turbines; T_{RH}: Temperature of reheat steam; T_{FG}: Temperature of flue gas; $p_{HP,IP,LP}$: Pressure of streams extracted from HP, IP and LP steam turbines; p_{CON}: Condenser pressure.

4.2. Supervisory control

The control system of a plant is usually divided into several layers, typically separated by different time scale requirements and objectives. Control architectures include regulatory control (seconds), supervisory control (minutes), local optimization (hours), site-wide optimization (days) and scheduling (weeks) [22]. Supervisory control can be designed to manipulate regulatory control set points and the remaining degrees of freedom of the plant (if any) to optimize the plant efficiency, within constraints imposed by the local controllers [46]. The critical first steps in designing a supervisor logic are to define the operational and economic objectives and the available degrees of freedom. Common degrees of freedom include the set points of the regulatory controllers, system boundaries not controlled and system parameters tunned to a particular operating scheme.

Figure 3 illustrates a scheme for such a supervisory control strategy for the power plant studied. The control system includes the supervisory control, regulatory control and plant level control. The regulatory control structure includes optimization controllers (marked as red dotted lines in Figure 1), which are the regulatory controllers used for plant optimization; and safety controllers (marked as black solid lines in Figure 1), which regulate the level of water in the drum, condenser and deaerator. The main function of the supervisory control is to update the set points of the optimization controllers ($\mathbf{y}_O^{sp}$), to maximize the plant efficiency of Eq.(1). The plant level controllers (marked with blue dashed lines in Figure 1) adjust the mass flow rates of coal, preheated air and feedwater according to the market power demand ($\mathbf{y}_P^{sp}$). The set points of the control system include the set points of the safety controllers, plant-level controllers and optimization controllers, i.e. $\mathbf{y}^{sp} = \{\mathbf{y}_S^{sp}, \mathbf{y}_P^{sp}, \mathbf{y}_O^{sp}\}$. These controllers manipulate control inputs ($\mathbf{u} = \{\mathbf{u}_S, \mathbf{u}_P, \mathbf{u}_O\}$) to maintain the controlled variables at their set points. In principle, one should consider disturbance ($\boldsymbol{\omega}^x$) and measurement noise ($\boldsymbol{\omega}^y$), which are responsible for a difference ($\mathbf{e}$) between model ($\mathbf{y}^{pred}$) and power plant outputs ($\mathbf{y}^{meas}$). An estimator could update model parameters ($\hat{\theta}$) and filter plant states ($\mathbf{x}$), to eliminate this model–plant mismatch. In this work, disturbance and measurement noise are not considered, mostly for reasons of simplifying the analysis, as the efficiency benefits are not affected by them (although the robustness of the supervisor will be). Therefore, $\boldsymbol{\omega}^x$ and $\boldsymbol{\omega}^y$ were considered negligible, and data filtering and state estimation (blocks in gray in Figure (3)) are not discussed. The supervisory control updates the optimal $\mathbf{y}_O^{sp}$ according to an objective function maximizing Eq.(1) in a formulation that includes the system model equations as discussed in the following.

Preprints (www.preprints.org) | NOT PEER-REVIEWED | Posted: 5 June 2018 doi:10.20944/preprints201806.0052.v1

Peer-reviewed version available at Processes 2018, 6, 114; doi:10.3390/pr6080114

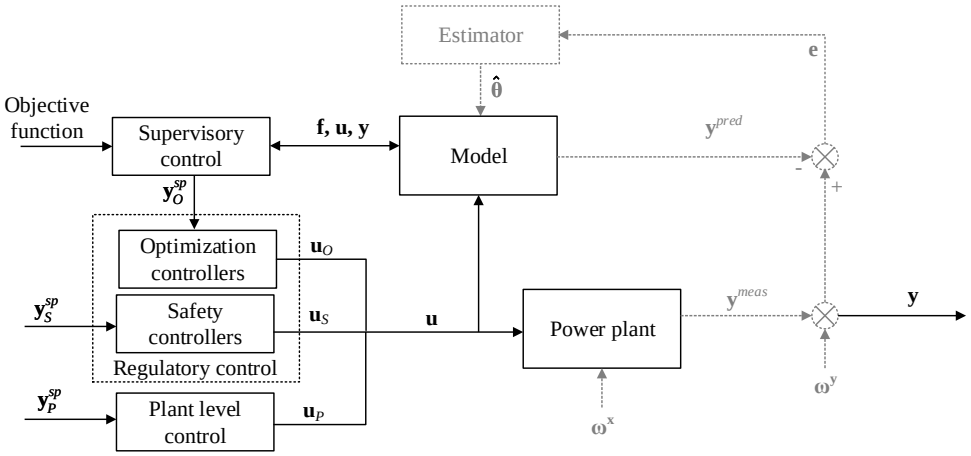

Figure 3. Multilayer control scheme for reheat regenerative cycle, 605 MW subcritical-pressure coal-fired power plant. $\mathbf{y}_O^{sp}$: Set points of the optimization controllers; $\mathbf{y}_S^{sp}$: Set points of the safety controllers; $\mathbf{y}_P^{sp}$: Set points of the plant level controllers; $\mathbf{u}_O$: Control inputs of the optimization controllers; $\mathbf{u}_S$: Control inputs of the safety controllers; $\mathbf{u}_P$: Control inputs of the plant level controllers; $\mathbf{u}$: Control inputs; $\boldsymbol{\omega}^x$: Disturbance; $\boldsymbol{\omega}^y$: Measurement noise; $\mathbf{y}^{pred}$: Predicted outputs; $\mathbf{y}^{meas}$: Measured outputs; $\mathbf{y}$: System outputs; $\mathbf{e}$: Error; $\hat{\boldsymbol{\theta}}$: Estimated model parameters; $\mathbf{f}$: System model.

4.3. Optimization formulation

As described previously, the set points of the optimization controllers are manipulated by the supervisory layer as first-level variables to improve plant efficiency (η), Eq.(1). This efficiency optimization also translates to coal consumption reduction and decrease of the plant carbon footprint. The intent of this work was to compare steady-state and dynamic optimization results of the plant of Figure 2 to those of the plant operating at nominal conditions. This comparison also includes an exploration of the added benefits of dynamic optimization, compared to those from steady state optimal operation. First, steady state optimization of the power plant operating at full load was performed by calculating optimal set points (constant with time) for the optimization controllers ($\mathbf{y}_O^{sp}$), and specifically the set points of the superheat steam temperature controller, preheat air temperature controller, and mass flow controllers of steam extracted from steam turbines. The steady state optimization problem formulation is shown in Eq.(2):

$$
\begin{aligned}
&\max_{\mathbf{y}_O^{sp}} \eta(\mathbf{y}, \mathbf{u}_P) \\
&\text{subject to:} \\
&\mathbf{f}(\mathbf{x}, \mathbf{u}, \boldsymbol{\theta}) = 0, \\
&\mathbf{u} = \mathbf{F}(\mathbf{y}_O^{sp}, \mathbf{y}) \\
&\mathbf{y} = \mathbf{h}(\mathbf{x}, \mathbf{u}, \boldsymbol{\theta}), \\
&\mathbf{x}^{min} \leq \mathbf{x} \leq \mathbf{x}^{max}, \\
&\mathbf{u}^{min} \leq \mathbf{u} \leq \mathbf{u}^{max}, \\
&\mathbf{y}^{sp,min} \leq \mathbf{y}^{sp} \leq \mathbf{y}^{sp,max}, \\
&\mathbf{y}^{min} \leq \mathbf{y} \leq \mathbf{y}^{max},
\end{aligned}
\tag{2}
$$

where the plant efficiency η is a function of power plant outputs ($\mathbf{y}$) and admissible variable values ($\mathbf{u}_P$) determined by the updated regulatory controllers level controller set points $\mathbf{y}_O^{sp}$; $\mathbf{f}(\cdot)$ is the vector of steady state equations describing the system in terms of states, $\mathbf{x}$, admissible inputs, $\mathbf{u}$, and parameters,

θ; and $\mathbf{F}$ describes the control functions, with $\mathbf{y}$ being the measured system outputs, mapped to $\mathbf{x}$, $\mathbf{u}$, and θ through $\mathbf{h}(\cdot)$.

Dynamic optimization was performed for the reference power plant operating under a time-varying power demand normalized from the New England area data [30]. The objective was to maximize the integral of plant efficiency over a predetermined time horizon, τ. This was accomplished by calculating time-varying optimal set points for the optimization controllers. The generic formulation of the dynamic optimization problem solved for the power plant of Figure (1) is presented in Eq.(3), where $\mathbf{f}$ is the system of differential algebraic equations describing the conservation of mass and energy, $\mathbf{x}$ is the vector of temporal state variables, $\mathbf{x}^0$ is the vector of initial state variables, $\mathbf{y}_O^{sp}$ is the temporal set points of the optimization controllers, $\mathbf{y}$ are the temporal system outputs, $\mathbf{t}_n$ is the vector of control action time points, with constant interval, τ_n, τ is the optimization horizon, and t is the time.

$$
\begin{aligned}
&\max_{\mathbf{y}_O^{sp}(\mathbf{t}_n)} \int_0^{\tau} \eta(\mathbf{y}_O^{sp}(t), \mathbf{u}_P(t))dt \\
&\text{subject to:} \\
&\mathbf{f}(\dot{\mathbf{x}}, \mathbf{x}, \mathbf{u}, \theta, t) = 0, \\
&\mathbf{u} = \mathbf{F}(\mathbf{y}_O^{sp}(\mathbf{t}_n), t), \\
&\mathbf{y} = \mathbf{h}(\mathbf{x}, \mathbf{u}, \theta, t), \\
&\mathbf{x}(t=0) = \mathbf{x}^0, \\
&\mathbf{x}^{min} \leq \mathbf{x} \leq \mathbf{x}^{max}, \\
&\mathbf{u}^{min} \leq \mathbf{u} \leq \mathbf{u}^{max}, \\
&\mathbf{y}^{sp,min} \leq \mathbf{y}^{sp} \leq \mathbf{y}^{sp,max}, \\
&\mathbf{y}^{min} \leq \mathbf{y} \leq \mathbf{y}^{max}, \\
&t \in [0, \tau],\ \mathbf{t}_n \in [0, \tau],
\end{aligned}
\tag{3}
$$

Table 3 shows optimization variables bounds and time interval constraints for the problems of Eqs. (2–3) of the two cases studied. The set points of the controllers regulating T_{SH}, T_{Air}, and $\dot{\mathbf{m}}_{ST}$ (including $\dot{m}_{IP1}$, $\dot{m}_{IP2}$, $\dot{m}_{LP1}$ and $\dot{m}_{LP2}$) were manipulated by the supervisory control layer as degrees of freedom seeking for an optimal input. In Case study I, only the set points of T_{SH} and T_{Air} were manipulated. Although not shown in Fig. 2, preheating of the air fed to the combustor to T_{Air} was accomplished by manipulating the mass flow of the Economizer exhaust gas sent to the air preheater (with the balance being waste heat). In Case study II plant optimization was performed by manipulating the set points of $\dot{\mathbf{m}}_{ST}$, i.e. the set points of the mass flow rates of steam streams extracted from the first IP turbine (IP1), the second IP turbine (IP2), the first LP turbine (LP1), and the second LP turbine (LP2) ($\dot{m}_{IP1}$, $\dot{m}_{IP2}$, $\dot{m}_{LP1}$, and $\dot{m}_{LP2}$, respectively). The ranges of the admissible inputs, shown in Table 3, are based on common practice and previous work [13–15,27,36,38,41–43,45]. The optimization horizon, τ, was set to 24 hours in Case study I and 4 hours in Case study II, and the control action interval, τ_n, was set to 1 hour. Large control actions where not penalized in the optimization problems solved, as the plant load profiles matched during the real-time plant optimization were relatively smooth. For instance the temperature of the superheated steam feeding the steam turbine was seen to change gradually over time in response to load changes, which is adequate for the protection of the steam turbines by thermal stress [14,36].

Table 3. Inputs for the optimization problems studied.

Case I				
Admissible inputs ($\mathbf{y}_O^{sp}$)	T_{SH}^{sp}(°C)		T_{Air}^{sp}(°C)	
Min	520		150	
Max	610		250	
Case II				
Admissible inputs[a] ($\mathbf{y}_O^{sp}$)	$\dot{m}_{IP1}^{sp}$ (kg/s)	$\dot{m}_{IP2}^{sp}$ (kg/s)	$\dot{m}_{LP1}^{sp}$ (kg/s)	$\dot{m}_{LP2}^{sp}$ (kg/s)
Min	16	10	10	28
Max	28	28	28	47
Temporal inputs[b]				
$\tau_n(hr)$	1			
$\tau(hr)$	24 for Case I (4 for Case II)			

[a] $\dot{m}_{IP1}$: Mass flow rate of steam stream extracted from IP1 turbine; $\dot{m}_{IP2}$: Mass flow rate of steam stream extracted from IP2 turbine; $\dot{m}_{LP1}$: Mass flow rate of steam stream extracted from LP1 turbine; $\dot{m}_{LP2}$: Mass flow rate of steam stream extracted from LP2 turbine; sp: Set point.
[b] If the plant is operating under time-varying power load.

5. Results

For each case study in the following, the static optimization of the power plant operating at full load with the optimization formulation of Eq.(2) is discussed first, followed by the dynamic optimization of the power plant operating under time-varying power load with the optimization formulation of Eq.(3). In the results discussed in the floowing, the power plant was formulated with the object-oriented language Modelica [20], in the commercial software Dymola [16] and set point optimization was performed in Matlab [47] using an interior-point algorithm. Model exchange between the software packages of Dymola and Matlab was accomplished with use of the Functional Mockup Interface, a tool-independent standard for seamlessly integrating models in various simulation environments [48].

5.1. Case study I: optimization variables T_{SH} and T_{Air}

Table 4 presents steady state optimization results at full load using the superheated steam temperature set point, T_{SH}^{sp}, and that of the preheat air temperature, T_{Air}^{sp}, as the optimization variables. Manipulation of T_{SH}^{sp} and T_{Air}^{sp} led to a power plant efficiency improvement from 38.3% to 40.23%. This efficiency improvement translates to fuel savings of 3.78%, with the fuel flow rate decreasing from 56.38 kg/s to 54.25 kg/s. The carbon footprint of the plant also decreased from 0.8 kg/kWh to 0.77 kg/KWh. This efficiency optimization was accomplished by increasing T_{Air} from 200°C to 248°C, and increasing T_{SH} from 538°C to 560°C. This is consistent with earlier reports [13,14,27,38,41–43], showing that increasing T_{SH} and T_{Air} translates to efficiency improvements. The higher T_{SH} enables the HP turbine to produce the same mechanical torque at lower coal consumption, while increasing T_{Air} recovers more waste heat from the boiler exhaust gas. It should be noted that the nominal steady state data used as baseline in Table 4, are as reported by Singer [29] for the reference power plant, and correspond to the design point of this plant. In principle the set points for T_{SH} and T_{Air} reported by Singer refer to an optimal plant configuration. The further improvement presented here could relate to better integrated plant-level optimization, model-plant differences and relaxation of plant constraints compared to the study reported in [29]. For an off–design operating point the efficiency benefits of solving Eq.(2) would, of course, have been much higher.

Table 4. Steady state optimization results of Case study I.

System output	Nominal	Optimal
T_{SH}^{sp} (°C)	538	560
T_{Air}^{sp} (°C)	200	248
η (%)	38.3	40.23
$\dot{m}_{Coal}$ (kg/s)	56.38	54.25
carbon footprint (kg/kWh)	0.8	0.77

The results of dynamic optimization for a horizon of 24 hours of plant operation are presented in Figure 4. Data and plant performance results are in response to time-varying power demand normalized from the New England area data [30] shown in Figure 4(a). In the absence of disturbances and and noise, the solution of Eq.(3) in the period $t = 0 - \tau (= 24hr)$ is equivalent to an off-line optimal control problem and is valid for the entirety of the time horizon considered. The optimization variables were T_{SH}^{sp} and T_{Air}^{sp}, but in this case they were updated in time intervals, $\tau_n = 1hr$. Figure 4 presents the dynamic power plant performance at nominal and optimal operation. The nominal dynamic operation is the result of constant T_{SH}^{sp} at 538°C and T_{SH}^{sp} at 200°C. Figures 4(d) and 4(e) show that the controlled variables, T_{SH} and T_{Air}, are robustly controlled at their optimal set points by the regulatory controller. The values of T_{SH} and T_{Air} from the dynamic optimization solution are always higher than their respective nominal values. In particular, Figure 4(d) shows that the optimal T_{SH}^{sp} trajectory is inversely proportional to that of the plant load. The optimal temporal T_{SH}^{sp} for a plant load higher than maximum, is higher than the 560°C of the optimal steady state at full load. This enhances heat transfer from the flue gas side to the steam side in the Superheater, at low plant load. Figure 4(e) shows that the optimal temporal profile of the temperature of air preheated by the flue gas exiting the boiler, is varying proportionally to plant load. The temperature of the exhaust gas is also proportional to the power load, due to the time-varying mass flow rates of feedwater, air and coal load. As Figure 4(c) shows, the improvement in time-averaged efficiency is 1.8% points. This efficiency improvement translates to coal savings of 184.8 tons/day (Figure 4(d)) and time-averaged carbon footprint decrease of 0.0351 kg/kWh (Figure 4(e)). In summary, the optimized power plant operates at higher $T_{Air}(t)$ and $T_{SH}(t)$, and this is consistent with the results of steady state optimization.

Preprints (www.preprints.org) | NOT PEER-REVIEWED | Posted: 5 June 2018 doi:10.20944/preprints201806.0052.v1

Peer-reviewed version available at Processes 2018, 6, 114; doi:10.3390/pr6080114

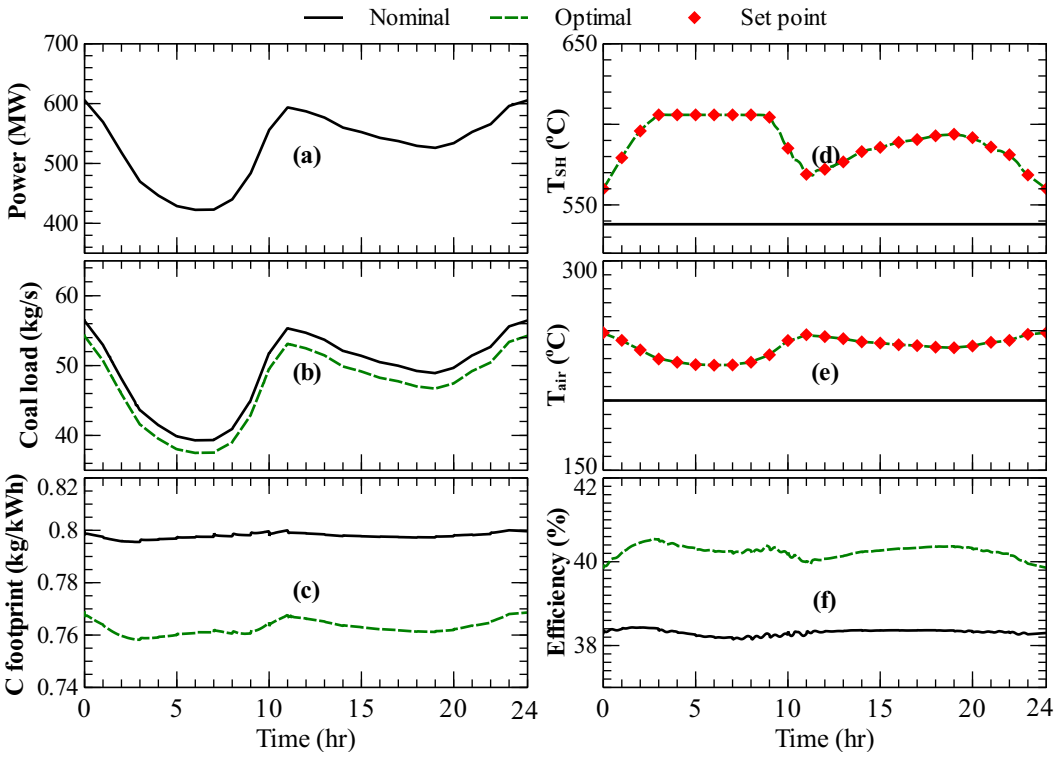

Figure 4. Dynamic optimization results of Case study I: (a) time-varying power load; (b) coal load; (c) carbon footprint; (d) temperature of preheated air; (e) temperature of superheated steam; (f) Power plant efficiency.

Figure 5 presents the dynamic performance of the power plant operating with constant nominal set points for T_{SH} and T_{Air}, constant optimal T^{sp}_{SH} and T^{sp}_{Air} (from the steady state optimization solution), and with time-varying optimal T^{sp}_{Air} and T^{sp}_{SH} (set by the dynamic optimization solution). The coal consumption and carbon footprint of the power plant operating with set points calculated by the static and dynamic optimization problem formulations are both lower than that by the power plant at nominal operation. The power plant operating with set points determined by dynamic optimization is the most efficient with the lowest coal consumption and the smallest carbon footprint. As shown in Table 5, the fuel savings accomplished by the power plant with steady state optimization are 160.9 tons/day, whereas the fuel savings accomplished with dynamic set point optimization are 184.8 tons/day. The reduction of coal load and decrease of carbon footprint of the dynamically optimal operation are pronounced when the power plant is operating at lower load. At different loads the plant has slightly different optimal regulatory control points compared to those of the steady state optimization at full load, which is exploited by the formulation of Eq.(3). As shown in Figure 4(d), the values of T^{sp}_{SH} calculated from Eq.(3) at low loads are higher than the constant T^{sp}_{SH} calculated from Eq.(2) at full load. Dynamically optimizing T^{sp}_{SH} improves the heat transfer in the Superheater at low loads and converts more heat from the superheated steam to mechanical torque. This increase in mechanical torque leads to improved power generation and efficiency. Moreover, the temperature profile of the preheated air in Figure 4(e) shows that the values of T^{sp}_{Air} calculated from Eq.(3) at low loads are lower than the constant T^{sp}_{Air} calculated from Eq.(2) at full load. At low loads, heat transfer between the water side and flue gas side in the boiler is enhanced, leading to lower flue gas temperatures, which in turn are to preheat the air. Thus, the supervisor drives T^{sp}_{Air} down to satisfy system constraints. Depending on the dynamic response times of the plant and the selection of the interval between control actions, τ_n, a multi-step steady state optimization problem could have resulted to similar performance benefits as those of Eq.(3). Nonetheless, Eq.(3) is more generic and robust for a dynamic system. It should be noted that one could execute the same analysis but with an objective function that maximizes

profit for varying electricity prices. This would have resulted in different plant load profiles, but the optimization procedure (not the objective function) and results would have been similar.

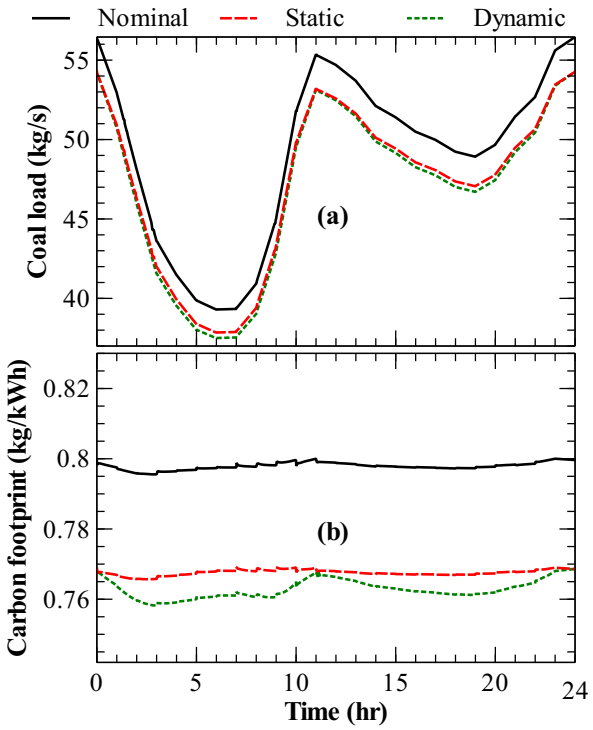

Figure 5. Comparison of the dynamic performance of the power plant with nominal operation set points, steady state optimal set points, and dynamic optimal set points: (a) coal load; (b) carbon footprint.

Table 5. Comparison of static and dynamic optimization of the power plant for Case study I.*

Output	Static optimization	Dynamic optimization
$\Delta\dot{m}_{coal}$ (tons/day)	160.9	184.8
$\Delta\bar{c}_f$ (kg/kWh)	0.0303	0.0351
$\Delta\dot{m}_{CO_2}$ (tons/day)	440.2	511.9

* $\Delta\dot{m}_{coal}$: Coal savings; $\Delta\bar{c}_f$: Decrease of the time-averaged carbon footprint; $\Delta\dot{m}_{CO_2}$: reduction of CO_2 emissions.

5.2. Case study II: Optimization variables $\dot{m}_{IP1}$, $\dot{m}_{IP2}$, $\dot{m}_{LP1}$ and $\dot{m}_{LP2}$

As shown in Figure 1, four proportional−integral (PI) controllers were used to regulate the mass flow rates of steam extracted from the turbines. The parameters of these controllers are presented in Table 6. These controllers manipulate the respective valves to regulate the mass flow rates of streams extracted from the IP1, IP2, LP1 and LP2 turbines. In this case study, the supervisory control variables are the set points of the mass flow controllers of steam extracted from turbines, namely the set points of $\dot{m}_{IP1}$, $\dot{m}_{IP2}$, $\dot{m}_{LP1}$, and $\dot{m}_{LP2}$.

Table 6. PI Controllers regulating the mass flow rates of steam extracted from turbines.

Controllers	IP1	IP2	LP1	LP2
Controlled variables	$\dot{m}_{IP1}$	$\dot{m}_{IP2}$	$\dot{m}_{LP1}$	$\dot{m}_{LP2}$
Manipulated variables	Valve opening	Valve opening	Valve opening	Valve opening
K_p	0.1	0.1	0.1	0.1
K_i	0.0001	0.0001	0.0001	0.0001

As before, steady state optimization was first performed for the plant operating at full load. The set points of $\dot{m}_{IP1}$, $\dot{m}_{IP2}$, $\dot{m}_{LP1}$ and $\dot{m}_{LP2}$ were manipulated by the supervisory control layer to maximize the plant efficiency of Eq.(2). The bounds of admissible inputs are shown in Table 3, with the optimal values presented in Table 7. The power plant efficiency was improved from 38.3% to 38.78%. The corresponding coal load decreased from 56.38 kg/s to 55.68 kg/s and the carbon footprint decreased from 0.8 kg/kWh to 0.79 kg/kWh. Compared with the nominal case, the optimal case has lower $\dot{m}^{sp}_{IP1}$, and higher $\dot{m}^{sp}_{IP2}$, $\dot{m}^{sp}_{LP1}$, and $\dot{m}^{sp}_{LP2}$, as shown in Table 7. The mass flow rate of steam extracted from the IP1 turbine is less than that of other steam turbine extractions. The IP1 turbine extraction has the highest pressure and temperature of all steam extractions. Thus, it is better utilized for electricity production than water preheating. Meanwhile, the steam extracted from IP2, LP1 and LP2 turbines is better utilized for preheating the condensed feedwater to reach higher temperature before entering the boiler. These results are consistent with the findings of the study by Chaibakhsh and Ghaffari [49] who proposed to reduce (or remove) the high pressure and temperature steam extraction stream and increase the steam extracted from the remaining IP and LP turbine stages.

Table 7. Steady state optimization results for Case study II.

System output	Nominal	Optimal
$\dot{m}^{sp}_{IP1}$ (kg/s)	27.4	16.8
$\dot{m}^{sp}_{IP2}$ (kg/s)	14	23.1
$\dot{m}^{sp}_{LP1}$ (kg/s)	16.5	23.7
$\dot{m}^{sp}_{LP2}$ (kg/s)	30	43.8
η (%)	38.3	38.78
$\dot{m}_{Coal}$ (kg/s)	56.38	55.68
carbon footprint (kg/kWh)	0.8	0.79

Dynamic optimization was performed for an optimization horizon of 4 hours. The interval 9–13 hr of the New England power demand data was used, as shown in Figure 6(a). In this interval the power plant is operating in response to a abrupt increase in power demand, with a power load change from 79.9% to 98.1%, followed by a decrease from 98.1% to 95.2%. This time interval includes the most abrupt change in power demand of the New England ISO data used, as well as a change in the sign of change in power demand. To solve this problem, the power plant model was first initialized to steady state at the load of 79.9% ($t = 0$ in Figure 6). As shown in Figure 6(a), the power generated by the plant model matches the time-varying power demand, which was accomplished by the plant load controllers shown in Figure 1.

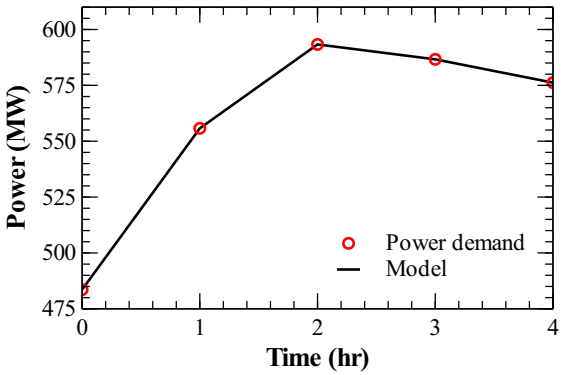

Figure 6. Time varying power demand and plant load for Case study II.

Figure 7 presents the transient operation of the virtual power plant in response to nominal inputs and to those calculated with dynamic optimization for the power plant load of Figure 6. The supervisor updated the set points of the controllers regulating $\dot{m}_{IP1}(t)$, $\dot{m}_{IP2}(t)$, $\dot{m}_{LP1}(t)$ and $\dot{m}_{LP2}(t)$, to seek for the maximum of the integral of efficiency over the time horizon of 4 hours. The nominal operation of the power plant corresponds to constant set points for the mass flow rate of turbine extraction streams, shown in Table 7. For the optimal dynamic operation, these set points were treated as dynamic optimization variables that are updated every hour by the supervisory controller. Figure 7(a) shows that the mass flow rate of the steam streams extracted from the turbines is robustly maintained at the respective temporal set points (updated in 1 hour intervals), set according to the dynamic optimization solution of the supervisor. Dynamic optimization requires the mass flow rate of IP1 steam extraction to be lower than that of the other steam extractions, similarly to the results from steady state optimization. The optimal mass flow rate of all the steam extraction streams follow the load profile. This is because the total mass flow rate of water circulating in the steam cycle is proportional to the power load. The improvement in the time-averaged efficiency is 0.43% points, as shown in Figure 7(b). Figures 7(c) and 7(d) show that the coal savings for four hours and the decrease of time-averaged carbon footprint are 7.72 tons and 0.00859 kg/kWh, respectively. These benefits become more profound at higher plant loads, which is in accordance to the relative contribution of the steam side of the plant to the overall power production.

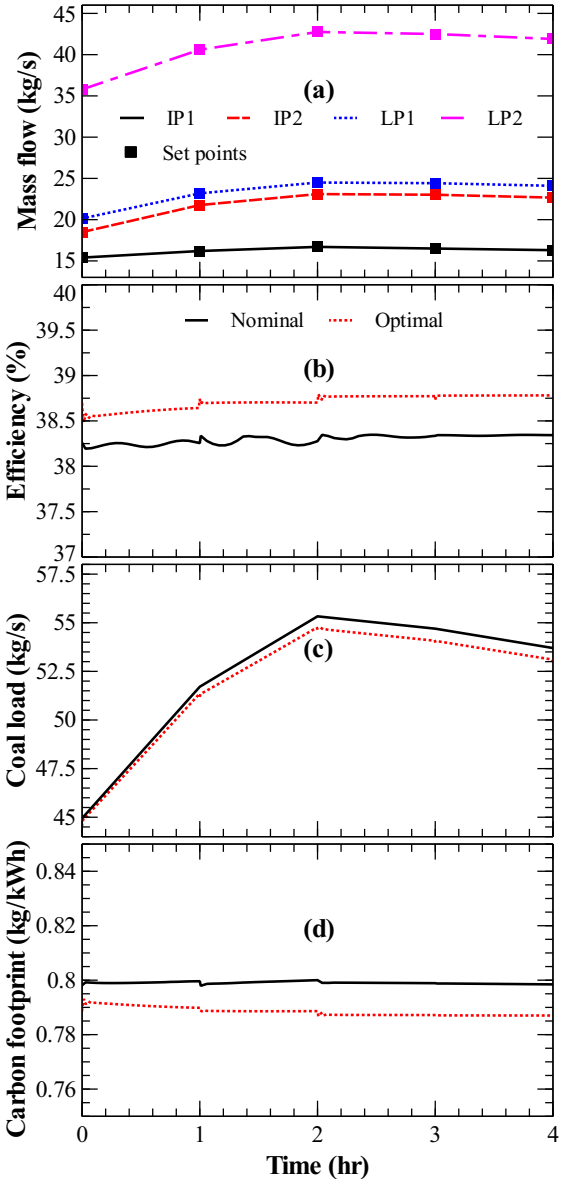

Figure 7. Dynamic optimization results of Case study II: (a) dynamic measurements and set points of mass flow rates of steam extracted from turbines; (b) coal load; (c) efficiency; (d) carbon footprint.

6. Conclusions

A dynamic power plant model was used as test-bed for dynamic simulation and optimization in response to variable plant load. Plant-level controllers were added to the plant model to meet a transient market power demand. Thereafter, optimization problems were formulated and solved with the objective to optimize power plant efficiency at steady state and dynamically. A supervisory control architecture was designed to manipulate the set points of regulatory controllers according to the solution of the optimization problems explored. The optimization variables T_{SH}^{sp} and T_{Air}^{sp}, and $\dot{\mathbf{m}}_{ST}^{sp}$, chosen in this work after a comprehensive literature review, enabled an improvement in time-averaged efficiency of up to 1.95% points with corresponding savings in coal consumption of 184.7 tons/day and carbon footprint decrease of 0.0352 kg/kWh. Comparison of the static and dynamic optimization formulations serving the supervisory controller showed that dynamic optimization offers higher time-averaged efficiency, fuel savings and CO_2 reduction.

Author Contributions: "Conceptualization, G.M.B. and C.C.; Methodology, G.M.B.; Software, C.C.; Validation, C.C.; Investigation, C.C.; Resources, G.M.B.; Writing—Original Draft Preparation, C.C.; Writing—Review & Editing, G.M.B.; Visualization, C.C.; Supervision, G.M.B.; Project Administration, G.M.B; Funding Acquisition, G.M.B."

Funding: This material is based upon work supported by the National Science Foundation under Grant No. 1054718.

Acknowledgments: CC gratefully acknowledges support by the GE Graduate Fellowship for Innovation and helpful advice and guidance from Alstom Power. This work was partially sponsored by the United Technologies Corporation Institute for Advanced Systems Engineering (UTC-IASE) of the University of Connecticut. Any opinions expressed herein are those of the authors and do not represent those of the sponsor.

Conflicts of Interest: "The authors declare no conflict of interest."

References

1. Han, L.; Bollas, G.M. Chemical-looping combustion in a reverse-flow fixed bed reactor. *Energy* **2016**, *102*, 669–681.
2. Han, L.; Bollas, G.M. Dynamic optimization of fixed bed chemical-looping combustion processes. *Energy* **2016**, *112*, 1107–1119.
3. Ibrahim, T.k.; Mohammed, M.K.; Awad, O.I.; Rahman, M.; Najafi, G.; Basrawi, F.; Abd Alla, A.N.; Mamat, R. The optimum performance of the combined cycle power plant: A comprehensive review. *Renewable and Sustainable Energy Reviews* **2017**, *79*, 459–474. doi:10.1016/j.rser.2017.05.060.
4. Viswanathan, R.; Henry, J.; Tanzosh, J.; Stanko, G.; Shingledecker, J.; Vitalis, B.; Purgert, R. U.S. Program on Materials Technology for Ultra-Supercritical Coal Power Plants. *Journal of Materials Engineering and Performance* **2005**, *14*, 281–292. doi:10.1361/10599490524039.
5. Hasler, D.; Rosenquist, W.; Gaikwad, R. New coal-fired power plant performance and cost estimates. *Sargent and Lundy Project* **2009**, pp. 1–82.
6. Cziesla, F. Lünen – State-of-theArt Ultra Supercritical Steam Power Plant Under Construction Andreas Senzel. Power Generation Europe, 2009, pp. 1–21.
7. U.S. Energy Information Administration. Energy Information Administration: Annual Energy Outlook 2018, 2018.
8. Masters, G.M. *Renewable and Efficient Electric Power Systems*; John Wiley & Sons, Inc.: Hoboken, NJ, USA, 2004; p. 712. doi:10.1002/0471668826.ch6.
9. Shah, R.; Mithulananthan, N.; Bansal, R. Oscillatory stability analysis with high penetrations of large-scale photovoltaic generation. *Energy Conversion and Management* **2013**, *65*, 420–429. doi:10.1016/j.enconman.2012.08.004.
10. Edmunds, R.; Davies, L.; Deane, P.; Pourkashanian, M. Thermal power plant operating regimes in future British power systems with increasing variable renewable penetration. *Energy Conversion and Management* **2015**, *105*, 977–985. doi:10.1016/j.enconman.2015.08.067.

11. Critz, D.K.; Busche, S.; Connors, S. Power systems balancing with high penetration renewables: The potential of demand response in Hawaii. *Energy Conversion and Management* **2013**, *76*, 609–619. doi:10.1016/j.enconman.2013.07.056.
12. Eser, P.; Singh, A.; Chokani, N.; Abhari, R.S. Effect of increased renewables generation on operation of thermal power plants. *Applied Energy* **2016**, *164*, 723–732. doi:10.1016/j.apenergy.2015.12.017.
13. Fu, C.; Anantharaman, R.; Jordal, K.; Gundersen, T. Thermal efficiency of coal-fired power plants: From theoretical to practical assessments. *Energy Conversion and Management* **2015**, *105*, 530–544. doi:10.1016/j.enconman.2015.08.019.
14. Sanpasertparnich, T.; Aroonwilas, A. Simulation and optimization of coal-fired power plants. *Energy Procedia* **2009**, *1*, 3851–3858. doi:10.1016/j.egypro.2009.02.187.
15. Tzolakis, G.; Papanikolaou, P.; Kolokotronis, D.; Samaras, N.; Tourlidakis, A.; Tomboulides, A. Simulation of a coal-fired power plant using mathematical programming algorithms in order to optimize its efficiency. *Applied Thermal Engineering* **2012**, *48*, 256–267. doi:10.1016/j.applthermaleng.2012.04.051.
16. Elmqvist, H.; Brück, D.; Otter, M. Dymola User's Manual, 1996.
17. Process Systems Enterprise. gPROMS Advanced User Guide, 2004.
18. Chen, C.; Han, L.; Bollas, G.M. Dynamic Simulation of Fixed-Bed Chemical-Looping Combustion Reactors Integrated in Combined Cycle Power Plants. *Energy Technology* **2016**, *4*, 1209–1220. doi:10.1002/ente.201600079.
19. Franke, R.; Babji, B.; Antoine, M.; Isaksson, A. Model-based online applications in the ABB Dynamic Optimization framework. Proceedings of the 6th International Modelica Conference, 2008, pp. 279–285.
20. Modelica Association. Modelica - A Unified Object-Oriented Language for Physical Systems Modeling, 2010.
21. Lind, A.; Sällberga, E.; Velutb, S. Start-up Optimization of a Combined Cycle Power Plant. Proceedings of the 9th International Modelica Conference, 2012.
22. Skogestad, S. Control structure design for complete chemical plants. *Computers & Chemical Engineering* **2004**, *28*, 219–234. doi:10.1016/j.compchemeng.2003.08.002.
23. Lestage, R.; Pomerleau, A.; Hodouin, D. Constrained real-time optimization of a grinding circuit using steady-state linear programming supervisory control. *Powder Technology* **2002**, *124*, 254–263. doi:10.1016/S0032-5910(02)00028-1.
24. Baillie, B.P.; Bollas, G.M. Development, Validation, and Assessment of a High Fidelity Chilled Water Plant Model. *Applied Thermal Engineering* **2017**, *111*, 477–488.
25. Mittal, K.; Wilson, J.; Baillie, B.; Gupta, S.; Bollas, G.; Luh, P.B. Supervisory Control for Resilient Chiller Plants under Condenser Fouling. *IEEE Access* **2017**, *5*, 14028–14046.
26. Sáez, D.; Ordys, A.; Grimble, M. Design of a supervisory predictive controller and its application to thermal power plants. *Optimal Control Applications and Methods* **2005**, *26*, 169–198. doi:10.1002/oca.757.
27. Ponce, C.V.; Sáez, D.; Bordons, C.; Núñez, A. Dynamic simulator and model predictive control of an integrated solar combined cycle plant. *Energy* **2016**, *109*, 974–986. doi:10.1016/j.energy.2016.04.129.
28. Chen, C.; Zhou, Z.; Bollas, G.M. Dynamic modeling, simulation and optimization of a subcritical steam power plant. Part I: Plant model and regulatory control. *Energy Conversion and Management* **2017**, *145*, 324–334.
29. Joseph, G.; Singer, P., Eds. *Combustion Fossil Power: A Reference Book on Fuel Burning and Steam Generation*, 4th ed.; Combustion Engineering: Windsor, Connecticut, 1991.
30. ISO New England. Real-time Maps and Charts, 2016.
31. Casella, F.; Leva, A. Modelica open library for power plant simulation: design and experimental validation. Proceeding of the 2003 Modelica Conference, 2003.
32. Hsu, C.; Chen, C. Applications of improved grey prediction model for power demand forecasting. *Energy Conversion and Management* **2003**, *44*, 2241–2249. doi:10.1016/S0196-8904(02)00248-0.
33. Akay, D.; Atak, M. Grey prediction with rolling mechanism for electricity demand forecasting of Turkey. *Energy* **2007**, *32*, 1670–1675. doi:10.1016/j.energy.2006.11.014.
34. Starkloff, R.; Alobaid, F.; Karner, K.; Epple, B.; Schmitz, M.; Boehm, F. Development and validation of a dynamic simulation model for a large coal-fired power plant. *Applied Thermal Engineering* **2015**, *91*, 496–506. doi:10.1016/j.applthermaleng.2015.08.015.

35. ABB and Rocky Mountain Institute. ABB Energy Efficiency Handbook: Power Generation – Energy Efficient Design of Auxiliary Systems in Fossil-Fuel Power Plants. Technical report, 2009.
36. Sanpasertparnich, T.; Aroonwilas, A.; Veawab, A. Improved Thermal Efficiency of Coal-Fired Power Station: Monte Carlo Simulation. 2006 IEEE EIC Climate Change Conference. IEEE, 2006, number 306, pp. 1–9. doi:10.1109/EICCCC.2006.277183.
37. Lizon-A-Lugrin, L.; Teyssedou, A.; Pioro, I. Appropriate thermodynamic cycles to be used in future pressure-channel supercritical water-cooled nuclear power plants. *Nuclear Engineering and Design* **2012**, *246*, 2–11. doi:10.1016/j.nucengdes.2011.07.024.
38. Suresh, M.V.J.J.; Reddy, K.S.; Kolar, A.K. Thermodynamic Optimization of Advanced Steam Power Plants Retrofitted for Oxy-Coal Combustion. *Journal of Engineering for Gas Turbines and Power* **2011**, *133*, 063001. doi:10.1115/1.4002251.
39. Suresh, M.; Reddy, K.; Kolar, A.K. ANN-GA based optimization of a high ash coal-fired supercritical power plant. *Applied Energy* **2011**, *88*, 4867–4873. doi:10.1016/j.apenergy.2011.06.029.
40. Wang, L.; Yang, Y.; Dong, C.; Morosuk, T.; Tsatsaronis, G. Multi-objective optimization of coal-fired power plants using differential evolution. *Applied Energy* **2014**, *115*, 254–264. doi:10.1016/j.apenergy.2013.11.005.
41. Xiong, J.; Zhao, H.; Zhang, C.; Zheng, C.; Luh, P.B. Thermoeconomic operation optimization of a coal-fired power plant. *Energy* **2012**, *42*, 486–496. doi:10.1016/j.energy.2012.03.020.
42. Koch, C.; Cziesla, F.; Tsatsaronis, G. Optimization of combined cycle power plants using evolutionary algorithms. *Chemical Engineering and Processing: Process Intensification* **2007**, *46*, 1151–1159. doi:10.1016/j.cep.2006.06.025.
43. Espatolero, S.; Cortés, C.; Romeo, L.M. Optimization of boiler cold-end and integration with the steam cycle in supercritical units. *Applied Energy* **2010**, *87*, 1651–1660. doi:10.1016/j.apenergy.2009.10.008.
44. Regulagadda, P.; Dincer, I.; Naterer, G.F. Exergy analysis of a thermal power plant with measured boiler and turbine losses. *Applied Thermal Engineering* **2010**, *30*, 970–976. doi:10.1016/j.applthermaleng.2010.01.008.
45. Kakaras, E.; Ahladas, P.; Syrmopoulos, S. Computer simulation studies for the integration of an external dryer into a Greek lignite-fired power plant. *Fuel* **2002**, *81*, 583–593. doi:10.1016/S0016-2361(01)00146-6.
46. Tatjewski, P. *Advanced Control of Industrial Processes*; Advances in Industrial Control, Springer London: London, 2007. doi:10.1007/978-1-84628-635-3.
47. The Mathworks Inc.. MATLAB, 2013.
48. Functional Mock-up Interface for Model Exchange, Version 1.0, 2010.
49. Chaibakhsh, A.; Ghaffari, A. Steam turbine model. *Simulation Modelling Practice and Theory* **2008**, *16*, 1145–1162. doi:10.1016/j.simpat.2008.05.017.